Published in final edited form as:
Ear Hear. 2011 ; 32(4): 436–444. doi:10.1097/AUD.0b013e3181ff33ab.

Identifying cochlear implant channels with poor electrode-neuron interface: electrically-evoked auditory brainstem responses measured with the partial tripolar configuration

Julie Arenberg Bierer, Ph.D., **Kathleen F. Faulkner, M.S.**, and **Kelly L. Tremblay, Ph.D.**

Abstract

Objectives—The goal of this study was to compare cochlear implant behavioral measures and electrically-evoked auditory brainstem responses (EABRs) obtained with a spatially focused electrode configuration. It has been shown previously that channels with high thresholds, when measured with the tripolar configuration, exhibit relatively broad psychophysical tuning curves (Bierer and Faulkner, 2010). The elevated threshold and degraded spatial/spectral selectivity of such channels are consistent with a poor electrode-neuron interface, such as suboptimal electrode placement or reduced nerve survival. However, the psychophysical methods required to obtain these data are time intensive and may not be practical during a clinical mapping procedure, especially for young children. Here we have extended the previous investigation to determine if a physiological approach could provide a similar assessment of channel functionality. We hypothesized that, in accordance with the perceptual measures, higher EABR thresholds would correlate with steeper EABR amplitude growth functions, reflecting a degraded electrode-neuron interface.

Design—Data were collected from six cochlear implant listeners implanted with the HiRes 90k cochlear implant (Advanced Bionics). Single-channel thresholds and most comfortable listening levels were obtained for stimuli that varied in presumed electrical field size by using the partial tripolar configuration, for which a fraction of current (σ) from a center active electrode returns through two neighboring electrodes and the remainder through a distant indifferent electrode. EABRs were obtained in each subject for the two channels having the highest and lowest tripolar (σ=1 or 0.9) behavioral threshold. Evoked potentials were measured with both the monopolar (σ=0) and a more focused partial tripolar (σ ≥ 0.50) configuration.

Results—Consistent with previous studies, EABR thresholds were highly and positively correlated with behavioral thresholds obtained with both the monopolar and partial tripolar configurations. The Wave V amplitude growth functions with increasing stimulus level showed the predicted effect of shallower growth for the partial tripolar than for the monopolar configuration, but this was observed only for the low threshold channel. In contrast, high-threshold channels showed the opposite effect; steeper growth functions were seen for the partial tripolar configuration.

Conclusions—These results suggest that behavioral thresholds or EABRs measured with a restricted stimulus can be used to identify potentially impaired cochlear implant channels. Channels having high thresholds and steep growth functions would likely not activate the appropriate spatially restricted region of the cochlea, leading to suboptimal perception. As a clinical tool, quick identification of impaired channels could lead to patient-specific mapping strategies and result in improved speech and music perception.

Correspondence to: Julie Arenberg Bierer, 1417 N.E. 42nd Street, Box 354875, Dept. of Speech and Hearing Sciences, University of Washington, Seattle, WA 98105, phone: 206-543-6640, facsimile: 206-543-1093, jbierer@u.washington.edu.

Keywords

Auditory brainstem response; cochlear implant; electrode configuration; partial tripolar

INTRODUCTION

The cochlear implant has provided improved hearing for individuals with severe or profound hearing loss, yet there exists substantial variability in listening abilities (e.g., Koch et al., 2004). Although some studies have shown that implant performance can be partially accounted for by etiology and duration of deafness (Gantz et al., 1993; Gfeller et al., 2008), both of which are thought to reflect spiral ganglion neuron loss, a direct correlation between global spiral ganglion neuron survival and performance on speech tests has not been established (e.g., Nadol and Eddington, 2006). Nevertheless, patterns of local neuron degeneration may reduce the effectiveness of auditory nerve stimulation by individual implant electrodes, which can indirectly affect performance (Khan et al., 2005; Fayad and Linthicum, 2006). Other local factors, such as the electrode position within the cochlea and bone and tissue growth, may also have a negative impact on what we refer to as the *electrode-neuron interface*. Here we examine if electrically-evoked auditory brainstem responses (EABRs) can be used to identify cochlear implant channels with a poor electrode-neuron interface.

Previous results from our laboratory and others have indicated that high variability in thresholds measured across the electrode array of individual subjects is a predictor of poor performance on speech tests (Pfingst et al., 2004; Bierer, 2007; Long et al., 2010). The channel-to-channel variability was higher for focused electrode configurations, such as bipolar, tripolar, and phased-array, than for the broader monopolar configuration. These results are consistent with focused configurations having a greater sensitivity to the electrode-neuron interface, which we define as an implant channel's ability to activate the auditory nerve. Factors such as the radial distance between the implant electrodes and the osseous spiral lamina, the numbers and distribution of viable spiral ganglion neurons, the stimulability of those neurons (including the role of peripheral processes), and bone and tissue growth within the scala tympani, may all impact the electrode-neuron interface. In a recent cochlear implant model of focused stimulation (Goldwyn et al., In press), channels having a poor electrode-neuron interface had higher thresholds and, produced broader activation patterns of auditory neurons along the cochlea. Such an association between high thresholds and broader spatial activation has been corroborated behaviorally using psychophysical tuning curve measures (Bierer and Faulkner, 2010). Broad spatial activation could result in the distortion of spectral cues because a signal delivered by a degraded channel may activate neurons beyond the targeted population of neurons. Therefore, identification of channels with a poor electrode-neuron interface might provide some insight into the variability in speech perception abilities across implant listeners.

EABRs may be a sensitive tool for identifying channels with a poor electrode-neuron interface. Previous studies in animal models have shown a relationship between the degree of spiral ganglion loss and evoked potential measures (Smith and Simmons, 1983; Hall, 1990; Shepherd et al., 1993; Miller et al., 1994; Miller 2008 review). In those studies, the aspect of the EABRs having the strongest correlation to neural loss was the slope of the amplitude growth function, assumed to be proportional to the number of responding nerve fibers. It is unclear what impact localized spiral ganglion cell loss might have had on the EABR responses in these studies, because only global cell counts were made. However, in one of the studies a significant correlation was measured only when the implant electrodes were placed relatively close to the modiolus (Shepherd et al., 1993). These findings suggest

that EABRs may be sensitive to spiral ganglion loss and electrode-to-neuron distance, two important aspects of the electrode-neuron interface. Our modeling results (Goldwyn et al., In press) suggest that both of these factors (a large radial distance or a reduced local neuron count) have comparable influences on the spatial pattern of activated auditory neurons over a range of current levels: i.e. both result in patterns that are relatively broad at threshold and widen relatively faster with increases in current. Because the amplitude growth of an EABR with current reflects, in part, the recruitment of peripheral auditory neurons, the slope of this function should be greater for channels affected by a poor electrode-neuron interface.

In this study, EABRs were measured on channels suspected of having a good or poor electrode-neuron interface based on behavioral criteria established in our previous study (Bierer and Faulkner, 2010). Specifically, behavioral thresholds were measured across channels using the focused tripolar configuration, and the channels having the lowest and highest thresholds – hypothesized to have a good and poor electrode-neuron interface, respectively – were chosen for EABR testing. The perceptual and EABR measurements were made using both the monopolar configuration and the partial tripolar configuration, a hybrid of the monopolar and tripolar configurations in which a fraction of current from the active electrode returns through the adjacent pair of intracochlear electrodes and the remainder through an extracochlear electrode (e.g., Mens and Berenstein, 2005; Litvak et al., 2007). A fraction of zero is equivalent to MP, while a fraction of one is TP. The slopes of the EABR amplitude growth functions were compared across channels and configurations. In addition, growth functions were related to the behavioral thresholds and, for a subset of subjects, psychophysical tuning curves obtained in a previous study (Bierer and Faulkner, 2010). We hypothesized that channels with higher EABR thresholds would have steeper growth functions, consistent with our computer model (Goldwyn et al., In press) and preliminary results demonstrating steeper loudness growth for channels with high behavioral thresholds (Nye and Bierer, 2010). We also hypothesized that EABR amplitude functions would grow more gradually for a focused partial tripolar configuration than for the monopolar configuration, based on previous comparisons of monopolar and bipolar stimulation (e.g., Brown et al., 1996).

GENERAL METHODS

The electrode configurations used in this study include monopolar (MP), tripolar (TP), and partial tripolar (pTP). The MP configuration consists of an active intracochlear electrode and an extracochlear return electrode. The TP electrode configuration consists of an intracochlear active electrode, with the return current divided equally between each of the two nearest flanking electrodes (Jolly et al., 1996). The pTP configuration is also formed from three adjacent electrodes, but only a fraction of the return current, denoted by ‘σ’, is delivered to the flanking electrodes, with the remainder flowing to the distant extracochlear ground. Therefore, a σ of 0 is equivalent to MP (all current is directed to the extracochlear electrode), and a σ of 1 is equivalent to TP (no current is directed to the extracochlear electrode). Data analysis and plotting were performed in units of decibels relative to 1 mA. Compared to a linear scale, the decibel scale can better accommodate the large differences in current level requirements among configurations and across channels and subjects.

All stimulation levels used in these experiments were within the compliance limits supported by the implant. Based on the impedance values, the maximum compliance of active and return electrodes was calculated at the beginning of each test session based on an algorithm provided by Advanced Bionics Corp. (Advanced Bionics, personal communication). The compliance limit was defined as the maximum voltage supported by the device (8 V) divided by the impedance.

Subjects

Six adult cochlear implant listeners, five female and one male, participated in the study. All of the participants had been implanted with the HiFocus 1J electrode array, with center-to-center electrode distance of 1.1 mm, and the HiRes90k receiver-stimulator (Advanced Bionics Corp., Sylmar, CA). The six subjects ranged in age from 30 to 79 years, were native speakers of American English who had become deaf post-lingually, and had at least 9 months of experience with their implants. Pertinent subject demographics are shown in Table I, including current age, gender, duration of severe hearing loss, known etiology, and speech perception scores. The speech scores, based on the CNC words test at 65 dB SPL-A, were obtained in our laboratory within three months of the beginning of the experiment. The behavioral and EABR testing required 3 to 6 visits to the laboratory, with each session lasting from three to six hours. Each participant provided written consent, and experiments were conducted in accordance with guidelines established by the Human Subjects Division of the University of Washington.

Behavioral measures

Two sets of behavioral thresholds were obtained in this study. First, thresholds for all electrodes were measured with pulse trains in the TP configuration. The channels with the highest and lowest TP thresholds served as the experimental electrodes for the remainder of the study. An additional set of thresholds at a lower pulse rate were obtained using the MP configuration and a pTP configuration with an intermediate current fraction. This second set of thresholds allowed for direct comparisons between behavioral and EABR thresholds.

Tripolar thresholds to pulse trains—For each subject, thresholds were obtained for a 204 ms pulse train at a rate of 918 pulses per second for each electrode using the TP configuration (see Bierer and Faulkner, 2010 for details; a pTP current fraction of $\sigma = 0.9$ was necessary for three subjects in order to remain within the voltage compliance, but for simplicity we consider these data as “TP thresholds”). Pulse train thresholds for other configurations (MP, pTP with $\sigma = 0.5$) were also analyzed when those data were available from our previous study. The lowest and highest threshold channels obtained with the TP configuration for each subject were identified for further testing. All thresholds were measured with an adaptive two-down one-up, three-interval, three-alternative forced-choice procedure, which converges on the 70.7 percent correct point on the psychometric function (Levitt, 1971). Each run started at a suprathreshold level, and subjects responded using a mouse to indicate the interval that contained the signal. Twelve reversals (i.e., changes in the direction of the signal level) were measured for each trial, and the levels for the last eight were averaged and taken as threshold. For the first two reversals, the signal was adjusted in 2 dB steps; for the other 10 reversals, it was adjusted in 0.5 dB steps. If the threshold of two runs differed by more than 1 dB, a third run was collected and data from all three runs were averaged. The standard deviation for the last eight reversals from each run was measured; if the value exceeded 1 dB the subject was reminded that they could take a break, those data weren’t included and threshold was subsequently re-measured. The total number of trials per run was limited to 75.

All available channels were tested in this manner. Channels were deemed unavailable if they were not programmed in the patient’s clinical map because they were outside the cochlea or elicited a non-auditory or intolerable percept. Channels that were deactivated were also not included as return electrodes for the tripolar or partial tripolar configurations.

Monopolar and partial tripolar thresholds to low-rate pulses—Thresholds on the test channels were obtained using the same stimuli and methods used during EABR testing. The stimuli were 10, 102 μs/phase, biphasic, charge-balanced (cathodic phase first on the

active electrode) current pulses, presented at a rate of 11.1 pulses per second. Both the MP and pTP configurations were used. For each subject, the pTP fraction selected was one allowing for a reasonable growth of loudness from threshold to most comfortable level (MCL) or, if MCL could not be reached, to a level corresponding to at least a report of '3' on the loudness scale described below.

Most comfortable level—The MCL for each test channel was determined by presenting a suprathreshold version of the EABR stimulus (10, 102 μs/phase, biphasic, charge-balanced current pulses, presented at 11.1 pulses per second; pTP fraction was dependent on the subject) and asking the subject to adjust the level by clicking one of two options labeled "up" and "down." The subject was asked to set the level to the subjective rating of "loud but comfortable," corresponding to 7 on the 1–10 clinical loudness rating scale (0 'Off'; 1 'Just Noticeable'; 2 'Very Soft', 3 'Soft'; 4 'Comfortable but too Soft'; 5 'Comfortable but Soft'; 6 'Most Comfortable'; **7 'Loud but Comfortable'**; 8 'Loud'; '9 'Upper Loudness Limit'; 10 'Too Loud'; Advanced Bionics, 2003). The level was changed in 1 dB steps until the subject clicked the "down" button; thereafter it was changed in 0.5 dB steps. At least two runs were collected and averaged for each MCL condition. If the two measured MCLs differed by more than 1 dB, a third run was completed, and all three runs were averaged.

Psychophysical Tuning Curves (PTCs)—PTCs were obtained in four of the six subjects for whom the lowest and highest threshold channels were not at the end of the electrode array (S9, S22, S24, and S26). Methods used to obtain and quantify psychophysical tuning curve results are described in detail in Bierer and Faulkner (2010). Briefly, psychophysical tuning curves were measured using a forward masking paradigm in which the masker was a 204 ms pulse train with the configuration fixed at a pTP fraction of $\sigma = 0.5$. Thresholds and MCLs were measured to the masker stimulus (204 ms pulse train, $\sigma = 0.5$), to set the upper and lower limits for stimulation for each channel. The probe, a 10.2 ms pulse train fixed at 3 dB above the probe-alone threshold, was presented 9.18 ms after the masker. The level of the masker was adjusted to determine how much masking was required to just mask the probe. Masked thresholds were obtained using the same adaptive forced-choice tracking procedure as described above. The masker was presented in all three intervals, while the probe was presented randomly, but with equal probability, in only one of the three intervals. The subject was asked to indicate which interval sounded "different".

Quantifying PTCs—A unique aspect of the Bierer and Faulkner study was the use of a focused masker configuration of $\sigma = 0.5$, which allowed for comparisons of changes in tuning properties that are primarily a result of the varying probe configuration. To compute the slopes of the apical side of the PTCs, first the tip of the tuning curve (i.e., the lowest masker level required to mask the probe) was identified using normalized masker levels. Once the tip was identified, the level at which the curve crossed 80% of masker dynamic range was the endpoint in the apical direction. Then, using the raw data points from the tip through the endpoint, a least-square error line was obtained and its slope was calculated in decibels per millimeter. In the few cases where the tuning curve was shallow, such that the data did not fall below 80%, the minimum was used as the tip and the line was fit to the point where the data reached masker-alone MCL.

Electrically-Evoked Auditory Brainstem Responses (EABR)

The stimuli were 102 μs/phase, biphasic, charge-balanced (cathodic phase first on the active electrode) current pulses. Subjects were seated in a sound attenuated booth and asked to rest quietly or sleep with their eyes closed during each 3–4 hour test session. The stimuli were delivered to the implant using a clinical interface controlled by the Bionic Ear Data Collection System, version 1.15.158 (BEDCS, Advanced Bionics Corp., Sylmar, CA)

through a dedicated Platinum Series Processor. This PC based system controlled the timing of the stimulus presentations and delivered an external trigger to the evoked potential recording system (Neuroscan™). The amplifier was transiently blocked for 1 ms post-stimulus onset to prevent saturation from stimulus-related artifacts. Ag-AgCl electrodes were placed on the vertex (Cz - active), the mastoid of the ear contralateral to the implanted ear (M1/ M2 - reference) and the forehead (ground). The impedances of all recording electrodes were less than 2 kOhm. Recordings were bandpass filtered with a low-frequency cutoff of 100 Hz and a high-frequency cutoff of 3,000 Hz.

EABRs were measured in response to both MP and pTP stimulation, at a rate of 11.1 pulses per second, averaged over 1500 sweeps. Because the aim of the experiment was to evaluate the amplitude growth function, stimulus levels ranged from the behaviorally measured MCL to below threshold, in at least 5 steps. Initial stimulation levels were at or near MCL, and were decreased in large steps, until no response was detected, and additional levels were collected as time allowed. Two runs were collected for each stimulus level, with a third if movement was detected during online data collection. Preliminary data collection indicated that MP responses were more reliable, so MP was generally tested first to ensure that each subject had recordable responses. As a control, a no-stimulus EABR was also collected.

Post Processing—All artifacts exceeding ±15 mV were rejected from averaging. The recording window spanned 17 ms, 2-msec pre- and 15-msec post-stimulus time. After artifact rejection (±15mV), the remaining sweeps were averaged and 5-point smoothing was applied. The recordings were batch processed and converted to an ASCII format for further evaluation in Matlab (Mathworks, Natick, MA).

Wave V peaks and troughs were identified visually based on the latency, repeatability and decrease in amplitude with decreasing stimulus level. Each waveform was compared with that generated with a no-stimulus control run. Amplitudes were calculated based on the difference (in μV) between the positive peak and the following trough for Wave V. To estimate EABR threshold, the amplitude growth function of Wave V was interpolated to 100 points. The threshold was defined as the lowest current level for which the Wave V amplitude was at least 0.1 μV. These interpolated data were also used to estimate the slope of the growth function between threshold and the highest level tested for each condition.

RESULTS

Figure 1 displays the initial set of behavioral thresholds, measured at the higher pulse rate (918 pulses per second) for all subjects. Thresholds were obtained with tripolar for all available channels ($\sigma = 0.9$ or 1, as indicated), and partial tripolar ($\sigma = 0.5$) and monopolar ($\sigma = 0$) for some of the channels, as indicated by the symbols. Each panel represents data for one subject (denoted by the subject number in the top right or top left of the panel) as a function of cochlear implant channel number from apical to basal. The vertical dashed lines indicate the channels with the lowest and highest tripolar thresholds that were chosen for electrophysiological testing. As in previous studies, thresholds generally increased as the configuration became more focused, i.e. as the current fraction σ increased (e.g. Bierer and Faulkner, 2010). The channel-to-channel variability of threshold also increased with current fraction.

Complete EABR amplitude growth functions were measured for each subject for the two test channels in both the MP ($\sigma = 0$) and pTP conditions (σ ranging from 0.5 to 0.8). For each channel, the largest pTP fraction was used that provided some growth of loudness before the compliance voltage limit was reached. Example EABR waveforms from one subject are shown in Figure 2, for the channels with the lowest (A and B) and highest (C and

D) TP thresholds. For this example, MCL was reached for all stimulus conditions. The Wave V peak-to-trough amplitude was measured for each stimulus condition and is indicated by the filled triangles. Clear responses were obtained for the highest levels tested, and the response amplitude decreased as lower stimulus levels were used (top to bottom). In this case, the response amplitude at MCL is smaller for the high threshold channel for both electrode configurations tested (Fig. 2c and d).

The peak-to-trough amplitudes of Wave V as a function of stimulus level are plotted in Figure 3 for all subjects (top to bottom) for the lowest (left) and highest (right) threshold channels. The MP configuration is represented by black, with either open (low channel) or filled (high channel) symbols. The pTP configuration is represented by gray, with either striped (low channel) or filled (high channel) symbols. The pTP fraction used is indicated in the top right of each panel, and the numbers next to the symbols in the legend correspond to the subjects' 1-to−10 loudness ratings of the highest level tested, as described in the Methods section. The slope of each amplitude growth function was calculated from the least-square error line (shown in bold) fitting the data between the estimated threshold (stimulus level indicated by arrowhead below the abscissa) and the highest tested level.

The growth function slopes of low threshold channels increased more gradually for the pTP than the MP configuration, which is consistent with previous studies (Brown et al., 1996). In contrast, the opposite effect can be seen for the high threshold channels, such that the growth functions were often steeper for the partial tripolar configuration. The difference in growth function slope between MP and pTP configurations is plotted for the low (diagonal stripes) and high (stippled) threshold channels for each subject in Figure 4A. For this analysis, a positive number indicates the expected result that slopes with the MP configuration are steeper than those with the pTP configuration. For the channels with the lowest TP threshold the difference in slopes was positive for all six subjects, while for the channels with the highest TP threshold, the difference in slopes was negative for five of the six subjects (Wilcoxon signed rank test comparing channels with low and high thresholds, $p < 0.05$). Figure 4B displays the difference in growth function slope for the high and low threshold channels for the MP (open) and the pTP configurations (grey filled) for each subject. A positive number indicates that the slope was steeper for the high threshold channel, which was the finding with the pTP configuration for all six subjects. The distribution of results was variable for the MP configuration. A pairwise comparison of channels with low and high TP behavioral thresholds indicates a difference in amplitude growth functions for those channels (Wilcoxon signed rank test comparing slopes for high and low channels with MP and pTP configurations, $p < 0.05$)

EABR thresholds were compared to behavioral thresholds measured with the same low-rate pulse trains. Figure 5 plots behavioral thresholds (abscissa) as a function of EABR thresholds (ordinate) for the MP (left) and pTP (right) configurations. As in previous figures, the subject, stimulus configuration, and behavioral threshold status are represented by the symbol, color and fill, respectively. The EABR thresholds for the high- and low-threshold channels for each subject were not correlated so both data points were included in the regression analysis (Spearman rank correlation for MP, $r = 0.26$, $p = 0.65$, and for pTP, $r = 0.14$, $p = 0.8$). Across subjects, a statistically significant correlation was measured between these two threshold estimates for both electrode configurations (Spearman's rank correlation, MP, $r = 0.650$, $p = 0.02$; pTP, $r = 0.881$, $p < 0.001$).

Four of the six subjects had previously participated in the study by Bierer and Faulkner (2010), which measured psychophysical tuning curves for the lowest and highest threshold channels. (PTCs were not measured in the remaining two subjects because both the lowest and highest threshold channels were at the end of the electrode array (S29 and S30)). That

study demonstrated that the behavioral TP thresholds (i.e. the actual threshold current levels, not their categorical high/low status) were correlated with the sharpness of tuning, as quantified by the apical slope of the curves. Figure 6 indicates that the same relation holds with EABR thresholds. In this figure, the EABR thresholds were normalized by subtracting the average of the two test channels. The apical slope of the psychophysical tuning curve (ordinate) is plotted as a function of relative EABR threshold (abscissa) for the monopolar (left) and partial tripolar configurations (right). The PTC slopes for the high- and low-threshold channels for each subject were not correlated so both data points were included in the regression analysis (Spearman rank correlation for MP, $r = 0.60$, $p = 0.42$, and for pTP, $r = 0.0$, and $p = 1$). As with behavioral thresholds, higher EABR thresholds measured with the more focused configuration were predictive of broader tuning (Spearman's rank coefficient $r = -0.86$ and $p < 0.01$). The same trend exists for the monopolar data but the two measures were not correlated to statistical significance (Spearman's rank coefficient $r = -0.60$, $p = 0.12$).

DISCUSSION

The results of the present study suggest that, with spatially focused stimulation, EABR measures are sensitive to the same underlying factors that result in high and low behavioral thresholds. As expected, behavioral and EABR thresholds were strongly correlated for both the monopolar and partial tripolar configurations. However, only with the pTP configuration did the steepness of the EABR growth function depend on the behavioral classification of low- and high-threshold (TP) channels. Additionally, in subjects for whom psychophysical tuning curves were obtained, these same high-threshold channels exhibited relatively broad tuning. As discussed below, both the steeper EABR amplitude growth and broader psychophysical tuning imply a more extensive tonotopic activation of the cochlea. These results suggest that the measurement of behavioral or evoked potential thresholds using a focused electrode configuration could be an effective clinical tool to identify channels affected by a poor electrode-neuron interface.

Relation to previous studies

Consistent with previous findings, the estimates of EABR threshold were predictive of behavioral threshold when the same stimulus parameters were used, especially for the partial tripolar data (e.g. Brown et al., 1996). Generally, behavioral thresholds were slightly lower than EABR thresholds of individual channels, a finding that has also been shown previously (Brown et al., 2000). Although studies have demonstrated qualitative differences in EABR morphology based on apical to basal place of stimulation (Gallégo et al., 1996; Thai-Van et al., 2002; Firszt et al., 2002), no such differences were noted in the present set of experiments because we did not systematically choose the test electrodes based on cochlear location. We did, however, observe morphological differences between channels with low and high tripolar thresholds.

Previous comparisons of amplitude growth functions using the bipolar and monopolar configurations have reported shallower slopes for the more focused stimulation (Schindler et al., 1977; Black and Clark, 1980; Marsh et al., 1981; Abbas and Brown, 1991; Brown et al., 1996). This was not a general finding in the present study. Although we did observe shallower growth functions for the focused pTP configuration with the low-threshold test channels (6 of 6 subjects), the high-threshold TP test channels were actually steeper (5 of 6 subjects). This suggests a fundamental difference between channels having a high and low TP threshold, which supports our hypothesis that TP threshold reflects a channel's local interface with nearby neurons.

Two primary factors of the electrode-neuron interface are the position of the electrode in the cochlea and spiral ganglion neuron survival. Both factors can influence the TP and pTP thresholds that we measured behaviorally and physiologically. However, a number of animal studies indicate that these factors may have different effects on evoked potential growth. For instance, when electrode-neuron distance was systematically increased by moving the stimulating electrode toward the lateral wall of the scala tympani, EABR thresholds increased and growth functions became steeper (Shepherd et al., 1993). This finding is consistent with recent computer models showing that a large electrode-neuron distance, which results in broader tonotopic activation, leads to a faster recruitment of neurons with increasing current (Litvak et al., 2007; Goldwyn et al., In press). On the other hand, animal models of spiral ganglion survival have shown that reduced neuron survival results in elevated EABR thresholds but *shallow* amplitude growth functions (Hall, 1990; Shepherd et al., 1993). That is, the two types of electrode-neuron interface factors, both leading to high thresholds, nevertheless had opposite effects on amplitude growth. However, we believe that in these animal experiments, the pattern of spiral ganglion loss was global, because deafness was induced by an ototoxic drug administered uniformly throughout the basal turn of the cochlea (Hall, 1990; Shepherd et al., 1993). If this is true, then the broader tonotopic activation resulting from the higher current requirement was offset by the overall loss of neurons, causing slower neural recruitment and, therefore, a shallower growth function. In contrast, it is likely that the human subjects in the present study had a combination of global and localized neuron loss, as suggested by the high and variable TP thresholds across channels.

The implication that high TP thresholds reflect sub-optimal stimulation of a localized region of the cochlea is supported by the psychophysical tuning curve data measured in a subset of the subjects. The tuning curves had broader tuning for the test channels with high TP thresholds (Bierer and Faulkner, 2010). A tip-shift was also observed in some cases, which occurs when the degree of masking is greatest on a channel that is different than the probe channel. Analogous to acoustic studies of cochlear dead regions (e.g., Moore and Alcantara, 2001), the tip shifts provide further evidence that the high-threshold test channels were near regions of low-functioning auditory neurons. Importantly, the differences between the tuning curve properties for low- and high-threshold channels were more evident when a focused pTP configuration was used for the probe stimulus rather than the MP configuration (Bierer and Faulkner, 2010). Likewise, with the present EABR data, differences in threshold and amplitude growth between the low- and high-threshold test channels were also more pronounced with pTP stimulation.

Further support for a local neuron factor contributing to the differential effect of configuration on EABR amplitude growth comes from a recent computer modeling study. In that model, imposing a discrete region of spiral ganglion neuron loss adjacent to an electrode resulted in an elevated threshold and a steeper growth of neural recruitment with current (Goldwyn et al., In press; see also Bierer, In press). These effects were most evident for focused configurations. In particular, neural recruitment for the MP configuration was relatively invariant to electrode placement or the spatial extent of local neuron loss. Thus, the inconsistent effects of the MP configuration on EABR growth observed in the present study may be a reflection of this insensitivity to the local electrode-neuron interface.

The present study, as well as our previous modeling and psychophysical efforts, has primarily explored the spatial/spectral aspects of the electrode-neuron interface. But temporal factors may also be important. For example, animal studies have shown that the surviving spiral ganglion neurons following a period of deafness may exhibit degraded temporal fidelity and longer refractory periods (Shepherd and Javel, 1997; Shepherd et al., 2004; Vollmer et al., 2005). Also, there is recent evidence of a correlation between degraded

spatial and temporal resolution in cochlear implant listeners (Chatterjee and Yu, 2010). Therefore, to better understand the present findings in the context of underlying variability in the electrode-neuron interface, future studies should explore the contribution of temporal factors.

Clinical implications and future directions

The results of the present study, along with those of previous behavioral studies, suggest that the individual channels of a listener's cochlear implant array do not activate nearby spiral ganglion neurons equally well (Bierer and Faulkner, 2010). If a clear criterion could be developed as to what constitutes an ineffective channel – for example, one that considers channel selectivity, loudness growth, speech perception, etc – the identification of such channels could lead to an improved clinical mapping strategy, whereby each channel is programmed based on the presumed nature of the electrode-neuron interface.

Part of the motivation for using EABR measures in this study was to determine if such a tool would be sensitive enough to identify channels with a poor electrode-neuron interface. Although our study suggests that EABRs could be used for this purpose, it has also revealed practical limitations with this procedure. First, the ability to measure complete growth functions for multiple electrodes is more time consuming than a typical clinic visit. EABR testing for each electrode and each configuration required approximately 2 to 3 hours. To test all of the electrodes in this manner would be prohibitive in the clinic, especially for young children. For this reason, future experiments will explore the use of the electrically-evoked compound action potential (ECAP). ECAP measures are less time consuming than EABR measures because they require much fewer averages and the stimuli can be presented at a faster rate. Also, a recent study by Hughes and Stille (2008) demonstrates comparable measures with ECAP to psychophysical tuning curves. A major downside of the ECAP is that the response can be influenced not only by the way the stimulating electrode interfaces with local neurons, but also by the interface near the intracochlear recording electrode. The EABR, by virtue of its far-field scalp recording, reflects more of a whole-nerve response and may more closely reflect the interface of the stimulating electrode. In this respect, the EABR was a better physiological measure for preliminary evaluation of the electrode-neuron interface. Future studies will compare the EABR to ECAP responses obtained from different recording electrodes.

Acknowledgments

The authors would like to thank Leonid Litvak and the Advanced Bionics Corporation for technical support and for providing the research and clinical interfaces. And we thank the implant subjects, who spent many hours participating in this study, and Amberly Nye for collecting some of the data. This work was supported by the University of Washington Royalty Research Fund (JAB), the Virginia Merrill Bloedel Scholar award (KLT), the National Institutes of Health (NIDCD-R03 DC008883 – JAB, NIDCD- T32 DC005361 – KFF, NIDCD-R01 DC007705 – KLT, NIDCD P30 DC04661).

Sources of Support: University of Washington Royalty Research Fund (JAB) and Virginia Merrill Bloedel Scholar award (KLT), and National Institutes of Health (NIDCD- R03 DC008883 – JAB, T32 DC005361 – KFF, R01 DC007705 – KLT, P30 DC04661).

References

Abbas PJ, Brown CJ. Electrically evoked auditory brainstem response: growth of response with current level. Hear Res. 1991; 51:123–37. [PubMed: 2013539]

Bierer JA. Threshold and channel interaction in cochlear implant users: evaluation of the tripolar electrode configuration. J Acoust Soc Am. 2007; 121:1642–53. [PubMed: 17407901]

Bierer JA, Faulkner KF. Identifying cochlear implant channels with poor electrode-neuron interface: partial tripolar, single-channel thresholds and psychophysical tuning curves. Ear Hear. 2010; 31:247–58. [PubMed: 20090533]

Bierer JA. Probing the electrode-neuron interface with focused cochlear implant stimulation. Trends in Amp. In press.

Black RC, Clark GM. Differential electrical excitation of the auditory nerve. J Acoust Soc Am. 1980; 67:868–74. [PubMed: 6892642]

Brown CJ, Abbas PJ, Borland J, Bertschy MR. Electrically evoked whole nerve action potentials in Ineraid cochlear implant users: responses to different stimulating electrode configurations and comparison to psychophysical responses. J Speech Hear Res. 1996; 39:453–67. [PubMed: 8783126]

Brown CJ, Hughes ML, Luk B, Abbas PJ, Wolaver A, Gervais J. The relationship between EAP and EABR thresholds and levels used to program the nucleus 24 speech processor: data from adults. Ear Hear. 2000; 21:151–63. [PubMed: 10777022]

Chatterjee M, Yu J. A relation between electrode discrimination and amplitude modulation detection by cochlear implant listeners. J Acoust Soc Am. 2010; 127:415–26. [PubMed: 20058987]

Fayad J, Markarem A, Linthicum F Jr. Histopathologic assessment of fibrosis and new bone formation in implanted human temporal bones using 3D reconstruction. Otolaryngol Head Neck Surg. 2009; 141(2):247–252. [PubMed: 19643260]

Firszt JB, Chambers RD, Kraus N. Neurophysiology of cochlear implant users II: comparison among speech perception, dynamic range, and physiological measures. Ear Hear. 2002; 23:516–31. [PubMed: 12476089]

Gallego S, Micheyl C, Berger-Vachon C, Truy E, Morgon A, Collet L. Ipsilateral ABR with cochlear implant. Acta Otolaryngol. 1996; 116:228–33. [PubMed: 8725521]

Gantz BJ, Woodworth GG, Knutson JF, Abbas PJ, Tyler RS. Multivariate predictors of audiological success with multichannel cochlear implants. Ann Otol Rhinol Laryngol. 1993; 102:909–16. [PubMed: 8285510]

Gfeller K, Oleson J, Knutson JF, Breheny P, Driscoll V, Olszewski C. Multivariate predictors of music perception and appraisal by adult cochlear implant users. J Am Acad Audiol. 2008; 19:120–34. [PubMed: 18669126]

Goldwyn JH, Bierer SM, Bierer JA. Modeling the electrode-neuron interface of cochlear implants: effects of neural survival, electrode placement, and the partial tripolar configuration. Hear Res. In Press.

Hall RD. Estimation of surviving spiral ganglion cells in the deaf rat using the electrically evoked auditory brainstem response. Hear Res. 1990; 45:123–36. [PubMed: 2345111]

Hughes ML, Stille LJ. Psychophysical versus physiological spatial forward masking and the relation to speech perception in cochlear implants. Ear Hear. 2008; 29:435–52. [PubMed: 18344869]

Jolly CN, Spelman FA, Clopton BM. Quadrupolar stimulation for Cochlear prostheses: modeling and experimental data. IEEE Trans Biomed Eng. 1996; 43:857–65. [PubMed: 9216159]

Khan AM, Whiten DM, Nadol JB Jr, Eddington DK. Histopathology of human cochlear implants: correlation of psychophysical and anatomical measures. Hear Res. 2005; 205(1–2):83–93. [PubMed: 15953517]

Koch DB, Osberger MJ, Segel P, Kessler D. HiResolution and conventional sound processing in the HiResolution bionic ear: using appropriate outcome measures to assess speech recognition ability. Audiol Neurootol. 2004; 9:214–23. [PubMed: 15205549]

Levitt H. Transformed up-down methods in psychoacoustics. J Acoust Soc Am. 1971; 49(Suppl 2): 467. [PubMed: 5541744]

Litvak LM, Spahr AJ, Emadi G. Loudness growth observed under partially tripolar stimulation: model and data from cochlear implant listeners. J Acoust Soc Am. 2007; 122(2):967–981. [PubMed: 17672645]

Long, C.; Holden, T.; Parkinson, W.; Smith, Z.; van den Honert, C. Towards a measureof neural survival in recipients of cochlear implants: focused stimulation thresholds, speech understanding and electrode locations. 33rd Annual Midwinter research meeting of the Assoc. for Res. in Otolaryngology; Feb. 6–10; Anaheim, CA. 2010.

Marsh RR, Yamane H, Potsic WP. Effect of site of stimulation on the guinea pig's electrically evoked brain stem response. Otolaryngol Head Neck Surg. 1981; 89:125–30. [PubMed: 6784070]

Mens LH, Berenstein CK. Speech perception with mono-and quadrupolar electrode configurations: a crossover study. Otol Neurotol. 2005; 26(5):957–964. [PubMed: 16151343]

Miller CA, Abbas PJ, Robinson BK. The use of long-duration current pulses to assess nerve survival. Hear Res. 1994; 78:11–26. [PubMed: 7961173]

Miller CA, Brown CJ, Abbas PJ, Chi SL. The clinical application of potentials evoked from the peripheral auditory system. Hear Res. 2008; 242:184–97. [PubMed: 18515023]

Moore BC, Alcantara JI. The use of psychophysical tuning curves to explore deadregions in the cochlea. Ear Hear. 2001; 22(4):268–278. [PubMed: 11527034]

Nadol JB Jr, Eddington DK. Histopathology of the inner ear relevant to cochlear implantation. Adv Otorhinolaryngol. 2006; 64:31–49. [PubMed: 16891835]

Nye, AD.; Bierer, JA. Poor electrode-neuron interface demonstrated by steep growth of loudness with the partial tripolar configuration. 33rd Annual Midwinter research meeting of the Assoc. for Res. in Otolaryngology; Feb. 6–10; Anaheim, CA. 2010.

Pfingst BE, Xu L, Thompson CS. Across-site threshold variation in cochlear implants: relation to speech recognition. Audiol Neurootol. 2004; 9:341–52. [PubMed: 15467287]

Schindler RA, Merzenich MM, White MW, Bjorkroth B. Multielectrode intracochlear implants. Nerve survival and stimulation patterns. Arch Otolaryngol. 1977; 103:691–9. [PubMed: 588122]

Shepherd RK, Javel E. Electrical stimulation of the auditory nerve. I. Correlation of physiological responses with cochlear status. Hear Res. 1997; 108:112–44. [PubMed: 9213127]

Shepherd RK, Hatsushika S, Clark GM. Electrical stimulation ofthe auditory nerve: the effect of electrode position on neural excitation. Hear Res. 1993; 66:108–20. [PubMed: 8473242]

Shepherd RK, Roberts LA, Paolini AG. Long-term sensorineural hearing loss induces functional changes in the rat auditory nerve. Eur J Neurosci. 2004; 20:3131–40. [PubMed: 15579167]

Smith L, Simmons FB. Estimating eighth nerve survival by electrical stimulation. Ann Otol Rhinol Laryngol. 1983; 92:19–23. [PubMed: 6824273]

Thai-Van H, Gallego S, Truy E, Veuillet E, Collet L. Electrophysiological findings in two bilateral cochlear implant cases: does the duration of deafness affect electrically evoked auditory brain stem responses? Ann Otol Rhinol Laryngol. 2002; 111:1008–14. [PubMed: 12450176]

Vollmer M, Leake PA, Beitel RE, Rebscher SJ, Snyder RL. Degradation of temporal resolution in the auditory midbrain after prolonged deafness is reversed by electrical stimulation of the cochlea. J Neurophys. 2005; 93(6):3339–55.

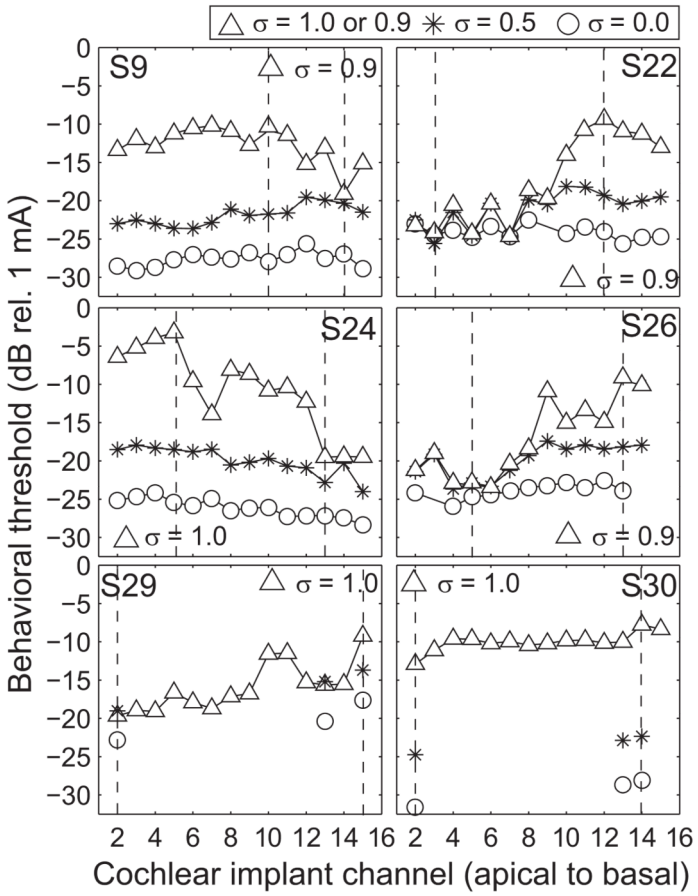

Figure 1.

Single-channel behavioral thresholds across subjects and configurations. Each panel plots the single-channel detection thresholds for a given subject (indicated in the top right corner). The abscissa represents cochlear implant channel from apical to basal and the ordinate represents detection threshold in decibels relative to 1 mA. Electrode configuration is indicated by symbols and for the triangles is either 0.9 or 1. The vertical dashed lines indicate the lowest and highest threshold channels obtained with the largest pTP fraction for each subject (0.9 for S9, S22, and S26 and 1.0 for S24, S29, and S30).

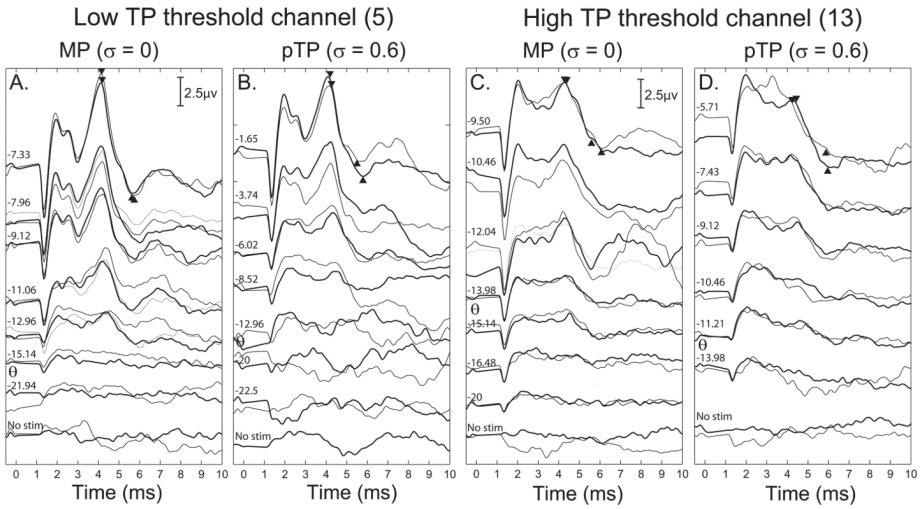

Figure 2.

Electrically-evoked auditory brainstem response (EABR) waveforms for the lowest (A, left two panels) and highest (B, right two panels) pTP threshold channels. The ordinate is response amplitude in μV and the abscissa is post-stimulus time in ms. Within each panel the EABR waveform is plotted with increasing stimulus levels from 0 current (bottom) to the most comfortable level (top) indicated at the left of each waveform. There are two waveforms plotted for each stimulus representing the replication of each waveform shown in black and grey lines. Within A and B, the left panels show responses to the MP configuration while the right panels show responses to pTP stimuli with a fraction of σ = 0.6. Data are from S26.

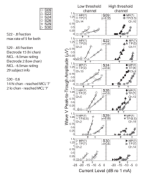

Figure 3.

Wave V amplitude growth functions for each subject and configuration. Amplitude was measured for Wave V of the EABR from the peak to the following trough in μV (ordinate) and is plotted as a function of stimulus level in dB (abscissa). The left and right columns are for the channels with low and high TP thresholds, respectively. Electrode configuration is indicated by black for MP and gray for pTP stimulus configurations. Data from the high and low threshold channels are indicated by the fill of the symbol (open or striped for the low threshold channels and filled for the high threshold channels). The pTP fraction used for each subject is indicated in the top right of each panel. In the legend for each panel the number in parentheses indicates the subjective rating of the loudness of the highest level tested for each stimulus configuration and channel. EABR threshold was taken as the level for which the amplitude growth function reached 0.1 μV and the current level at threshold is indicated by arrows below the abscissa. A least-square error best fit line is shown in bold from threshold to the highest tested level.

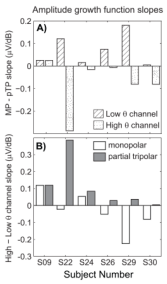

Figure 4.

A) The difference between amplitude growth function slopes (μV/dB) for monopolar and partial tripolar stimuli (abscissa) are shown for each subject for the low (diagonal stripes) and high (stippled) threshold channels. B) The difference between amplitude growth function slopes (μV/dB) for high and low threshold channels (abscissa) are shown for each subject for the MP (open) and pTP (grey filled) configurations.

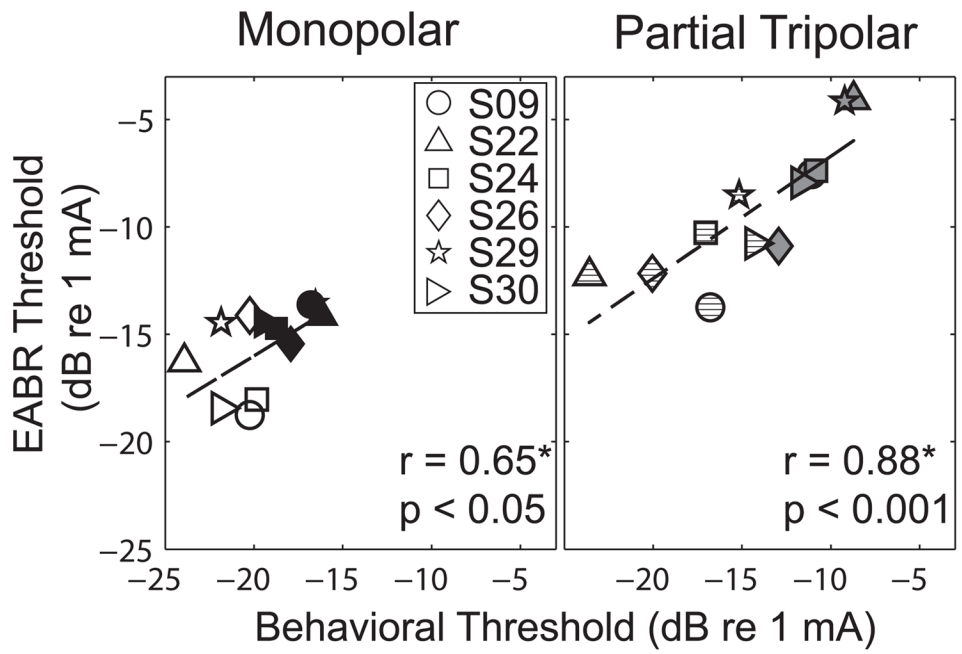

Figure 5.

Relation of behavioral threshold (abscissa) and EABR threshold (ordinate) for MP (left) and pTP (right) stimuli. As in previous figures, the symbol and fill of the data indicate the subject and the high or low threshold status of the channel, respectively. The solid line indicates a least-square error best fit line to the data. The statistics are based on the non-parametric Spearman's rank correlation coefficient.

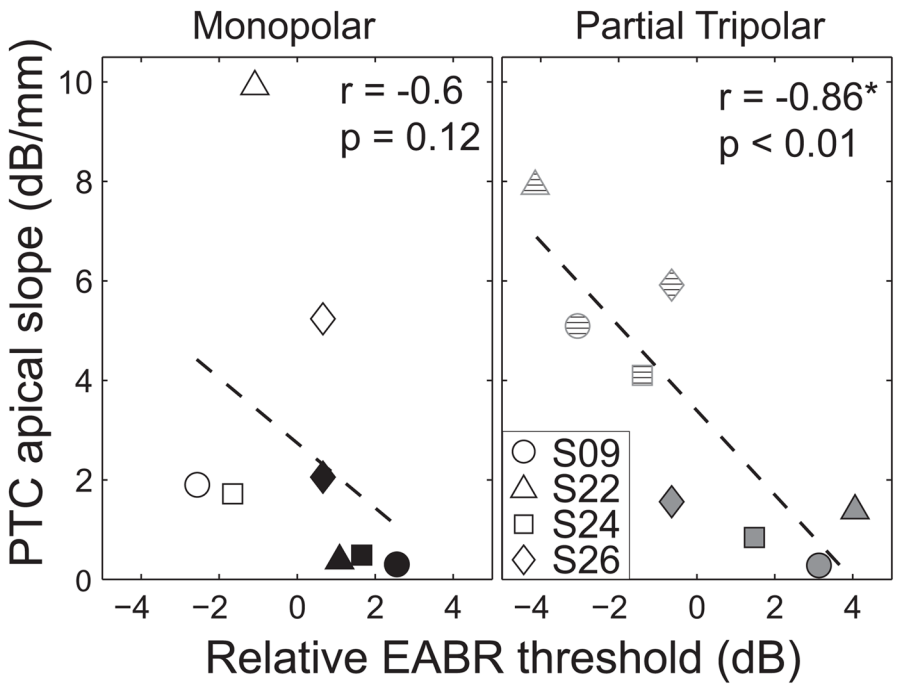

Figure 6.
Relation of the relative EABR threshold and sharpness of psychophysical tuning curves. EABR thresholds are relative to the average for each subject and are plotted on the abscissa. The apical slope of the psychophysical tuning curve in dB/mm is plotted on the ordinate. Symbol and fill indicate subject and electrode configuration. The solid line indicates a least-square error best fit line to the data. The statistics are based on the non-parametric Spearman's rank correlation coefficient.

Table 1

Subject Demographics

Subject Number	Sex	Age (years)	Duration of Severe Hearing Loss (years)	Duration of CI Use	Etiology of Hearing Loss	CNC Words in Quiet 65dB	CNC Phonemes in Quiet 65dB
S9	F	64	24	3 years	Hereditary	48%	75%
S22	F	67	12	9 months	Hereditary	68%	76%
S24	F	74	2	1 year	Unknown	54%	73%
S26	F	30	2	1.8 years	Atypical Menieres Disease	56%	78%
S29	M	79	32	2 years	Noise Exposure	60%	78%
S30	F	45	29	*16 years (2 years)	Hereditary	50%	75%

*S30 underwent reimplantation following a failure of the initial device and has two years experience with the reimplanted device.